

# Research on High Voltage Cable Condition Detection Technology based on Wireless Sensor Network

Yang Zhao<sup>\*1</sup>, Qing Liu<sup>2</sup>, Tong Shang<sup>3</sup>, Yingqiang Shang<sup>4</sup>, Rong Xia<sup>5</sup>, Shuai Shao<sup>6</sup>

State Grid Beijing Powercable Company, Beijing, 100022 China<sup>1,2,3,4</sup>

China Electric Power Research Institute Limited, Wuhan Branch, Wuhan, 430079 China<sup>5</sup>

Center of Jinan Power Supply Company of State Grid Shandong Electric Power Company, Jinan, 250012, China<sup>6</sup>

**Abstract**—The development and progress of modern society cannot be achieved without the support of electric power resources, and at present, electric power is the most important energy source to promote social development and maintain human life. As a key unit under the power distribution and transmission system, the high-voltage cable of the power grid will undertake the task of supplying power resources to the whole power grid. Therefore, based on the transmission line fault diagnosis framework of Wireless Sensor Networks (WSN), a high-voltage cable path condition monitoring scheme using LoRa technology is proposed. Three high-voltage cable condition monitoring periods are proposed according to the difference of high-voltage cable fault rate, and the delay and energy consumption of the high-voltage cable monitoring system are optimized by multi-objective particle swarm algorithm reality. The experimental results show that the proposed high-voltage cable detection technology can switch the working mode according to different environments, and the data communication packet loss rate is less than 5%, while the detection platform has excellent delay performance and energy saving effect. The high-voltage cable status detection solution can effectively solve the problem of blind high-voltage cable channels in high mountain areas of China. The research content has important reference value for the detection of China's power grid circuit system.

**Keywords**—Wireless sensor; high-voltage cable; fault diagnosis; particle swarm algorithm

## I. INTRODUCTION

Wireless sensor network is a kind of communication and acquisition network composed of nodes, which can realize the detection and acquisition of external physical energy. With the development of information and communication technology in recent years, wireless sensor networks have a wide range of applications in modern medical, industrial manufacturing, smart grid, etc. [1]. Wireless sensor network has the characteristics of bottom power consumption, simple application and easy expandability; therefore, wireless sensor network also has a very wide application in the field of smart grid power data acquisition, cable status monitoring, grid fault diagnosis, etc. [2-3]. With the advent of the information era, smart grid construction has become the new goal of China's power grid development. The United States as the representative of the developed countries on the future development of smart grid development strategy, which will be the wireless sensor network ZigBee protocol as an important communication standard for the construction of smart grid [4].

This shows that wireless sensor networks play an important role in the construction of smart grid. However, the construction of smart grid needs to meet the requirements of delay, bandwidth, reliability, and coverage, etc. The high-voltage grid is in a complex working environment, subject to harsh environment, complex weather, and interference from various electrical equipment signals, which will affect the application of wireless sensor networks [5]. Therefore, in view of the high difficulty in maintenance and repair of transmission lines in remote mountainous areas, a detection scheme for high-voltage cables in mountainous areas is proposed based on WSN technology. Different detection schemes are adopted for cables in different periods, and multi-objective particle swarm optimization algorithm is used to solve the problem, so as to solve the problem of high-voltage cable line fault detection in remote areas. The research content has important research value for the construction and development of smart grid in China.

Wireless sensor networks are widely used in modern medical, industrial manufacturing, smart grid, etc. A lot of work has been done by domestic and foreign researchers to study wireless sensor networks. Tabella et al. investigated the effect of wireless sensor networks (WSN) on oil spill detection and localization in subsea production systems. Four localization algorithms were studied and the detection and localization performance were compared with the (location) perspective chair Varshney's rule (CVR) and Cramér-Rao lower limit (CRLB), respectively. The results show that the components that would lead to leakage in case of failure and their corresponding failure rates [6]. Xf et al. found that the routing survivability in harsh environments is questionable. To address this issue, an environmental fusion multipath routing protocol (EFMRP) was proposed. The results show that EFMRP can significantly improve packet delivery rate and network lifetime in harsh environments [7]. Hu et al. found that a fully distributed time synchronization method based on Gaussian belief propagation would lead to degradation of synchronization accuracy. Thus, a Sequential Belief Propagation-based Distributed Time Synchronization algorithm (SBP-DTS) was proposed to reduce the number of Gaussian mixture components in messages using a weighted expectation maximization (EM) algorithm. Finally, the performance of SBP-DTS was evaluated under asymmetric Gaussian and exponential delay models [8]. Houssein et al. found it a challenging task to determine the location of convergence nodes in LSWSNs, and Harris' hawk's optimization (HHO)

algorithm was used to solve this problem. The results show that the adopted approach has advantages in terms of energy consumption and localization errors [9]. Lin et al. proposed a priority-aware packet transmission scheduling (PPTS) framework in a cluster-based IWSN, in which the PPTS policy, optimization theory, and implementation design are systematically considered. The results show that the proposed PPTS policy not only minimizes the transmission delay of high-priority packets but also improves the transmission delay of low-priority packets [10]. Zhan et al. propose an optimization problem that minimizes the weighted sum of the above two costs by optimizing the UAV trajectory and wake-up time allocation as well as the transmit power of all SNs. In addition, a new approach to design the initial UAV trajectory using the multi-traveler problem (MTSP) technique is proposed. The results show that the proposed design achieves a flexible trade-off in cost balance between UAVs and SNs [11]. Wang et al. propose a LEACH-EA protocol based on the LEACH algorithm for the low-power requirements of wireless sensor networks. Experiments show that the LEACH-EA protocol provides significant improvements in network life cycle, total network data transmission and number of cluster heads [12]. Verma et al. found limitations when using the battery power of sensor nodes. A fuzzy logic based effective clustering (FLEC) for homogeneous wireless sensor networks for mobile receivers is proposed. The probability of average energy is used to select the appropriate cluster head and the results show that the proposed FLEC scheme outperforms LEACH, DEEC and LEACH fuzzy protocols [13]. Jaber et al. proposed an “adaptive fully distributed duty cycle for content-centric wireless sensor networks (ADDC-CCWSN)” mechanism. The ADDC-CCWSN aims to reduce the activity of nodes with a high percentage of unsatisfied interest in the PIT. The results show that the proposed approach achieves significant energy efficiency gains while ensuring a high interest satisfaction rate and maintaining almost the same latency [14].

Neural network algorithms have a wide range of applications in the field of smart grid, providing important data support for data collection and grid diagnosis, and researchers at home and abroad have done a lot of work to study them. Yu et al. proposed a deep reinforcement learning algorithm for safe shutdown strategy in order to deal with incomplete distribution grid models to solve the voltage reactive power control problem in a model-free manner. The results show that the proposed algorithm outperforms existing reinforcement learning algorithms [15]. Pan E et al. used hierarchical cluster analysis to analyze grid influencing factors, and the results show that the prediction model is important to achieve accurate calculation of provincial enterprise investment [16]. Ying et al. proposed a coordinated scheduling method for plug-in electric vehicle PV generation microgrid based on extended power prediction, using a clustering algorithm to build the power prediction model was established and the results showed the good performance of the proposed extended coordinated scheduling algorithm [17]. Bhamidipati et al. developed Wide Area Monitoring Systems (WAMS) in order to monitor the grid in a wide area. And a new wide-area monitoring algorithm was developed to verify each substation

in an artificial intelligence framework. The results show that the Kullback-Leibler scatter-based method has fast detection time and the timing error estimation accuracy exceeds the limits provided by the IEEE C37.118.1-2011 standard [18]. Iliadis et al. developed a new algorithm for managing the currents of an islanded power system that enables more stable conventional unit operation and peak demand reduction. The results demonstrate that the proposed algorithm can achieve smoother diesel generator operation [19]. Jyotheeswara et al. proposed a neural network-based maximum power point tracking (MPPT) controller for PEMFC grid-connected systems to extract maximum power from proton exchange membrane fuel cells. The results show that the proposed RBFN-MPPT controller has excellent performance [20].

It can be seen from related domestic research that neural network algorithms have a wide range of applications in the field of smart grid. Optimization of wireless sensor network parameters by neural network algorithm is important to improve the monitoring effect of power grid cables.

## II. CONSTRUCTION OF HIGH-VOLTAGE CABLE CONDITION DETECTION MODEL BASED ON WIRELESS SENSOR NETWORK

### A. Mountain High Voltage Cable Path Loss Model Construction

Wireless sensor network is a wireless communication technology, and its low cost and maintenance-free characteristics make WSN technology gradually replace the backward wired monitoring scheme. Therefore, WSN technology will have a very broad application prospect in the field of smart grid. High-voltage cables in mountainous areas are susceptible to seasonal climate and harsh environment, and high-voltage cable faults are mainly concentrated in summer and winter time. To meet the requirements of monitoring high voltage cables in mountainous areas, transmission cable monitoring solutions need to meet the challenges of signal transmission, harsh environmental issues, and service life in mountainous areas. Therefore, based on wireless sensor network technology, an in-line monitoring system for high voltage cables in mountainous areas using LoRa is proposed. The high-voltage line transmission architecture is constructed by setting LoRa and cellular modules in the mountainous environment, and dynamic LoRa packet networking modules are set to guarantee the stable transmission of data signals as well as to improve the efficiency of system resources utilization and reduce system energy consumption. As shown in Fig. 1, the application principle of WSN in the field of smart grid.

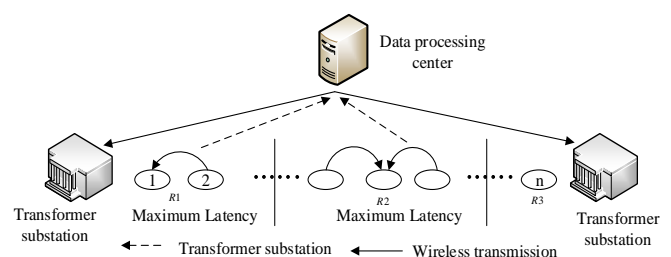


Fig. 1. Application principle of WSN in Smart Grid

According to the analysis of mountain high-voltage cable monitoring data, the probability of cable failure is different at different times, and mountain high-voltage cable monitoring is divided into three monitoring time periods. In the mountain storm season, snowstorm and frost season, when the relevant values are higher than the meteorological safety indicators, the occurrence of natural disasters around the mountain area of high-voltage cables is high, and the monitoring of mountain high-voltage cables is at the high-risk monitoring stage; natural disasters or abnormal communication signal transmission occur in the mountainous grid area, and the monitoring of mountain high-voltage cables is at the fault monitoring stage; cable monitoring data return to normal, and meteorological disasters gradually decrease, and mountain high-voltage cable monitoring is in the low-risk monitoring stage. According to the characteristics of the monitoring period, the fault stage gives priority to feedback data to the monitoring and issue fault maintenance orders; secondly, the high-risk stage feeds data to the monitoring and monitors the grid route fault problem; the low-risk stage only needs to meet the requirements of stable data transmission and cable detection. The signal strength of the transceiver module LoRa at a point in the mountainous area is expressed as the difference between the field strength of the system base station antenna and the field strength loss of the signal reaching that point, as seen in equation (1).

$$E_R = E_T - L_{PS} \quad (1)$$

In equation (1),  $L_{PS}$  represents the signal loss in the median path, and  $E_T$  represents the field generated by the LoRa antenna position of the transceiver module. During the transmission of the signal in the non-direct path, the bypassing phenomenon will occur, as shown in Fig. 2, then the bypassing path expression is seen in equation (2).

$$d_D = \sqrt{d_1^2 + (h_m - h_T)^2} + \sqrt{d_2^2 + (h_m - h_R)^2} \quad (2)$$

In equation (2),  $d_1$  indicates the distance between the mountain and the transceiver module,  $d_D$  indicates the signal bypass distance,  $d_2$  indicates the distance between the mountain and the antenna,  $h_R$  indicates the antenna altitude,  $h_T$  indicates the transceiver module altitude, and  $h_m$  indicates the mountain altitude.

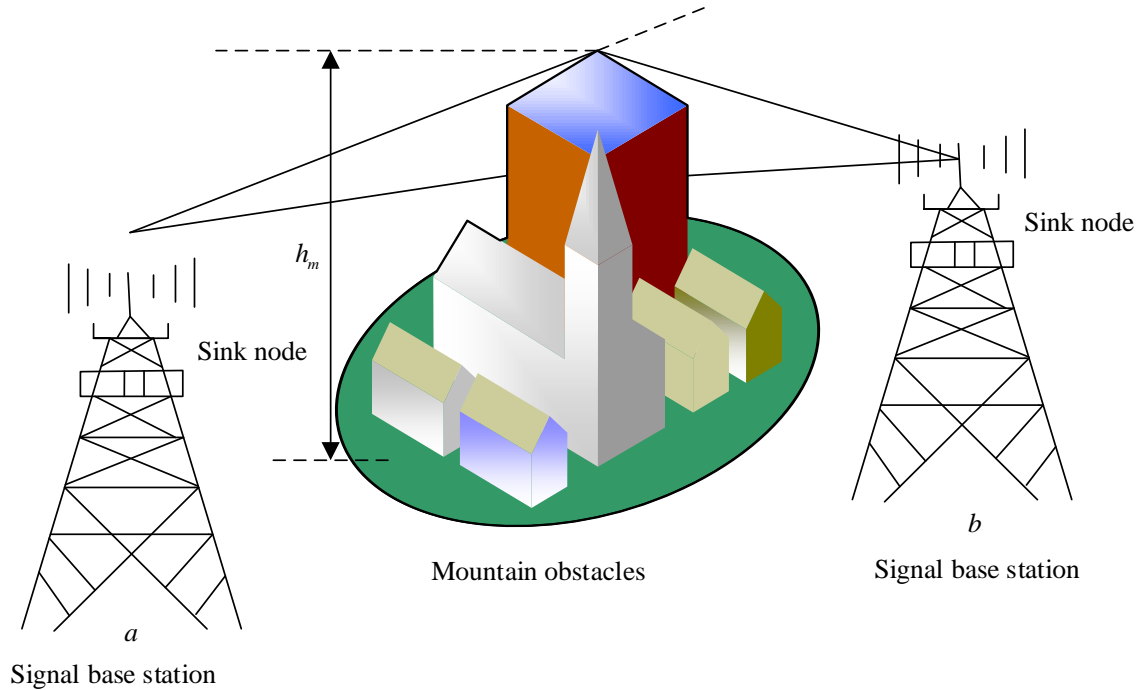


Fig. 2. Radio diffraction principle

The colored building areas in Fig. 2 represent signal blocking areas such as mountains and forests. The signal tower transmitting signal is blocked by the mountain and signal bypassing phenomenon occurs. The transceiver module LoRa signal band is 433-915Mhz, to meet the bypass signal loss requirements, the model applicable to the loss monitoring in this band is Egli model, which can be more accurate to evaluate the terrain field strength in mountainous and hilly

areas, etc. The Egli signal loss expression is seen in equation (3).

$$L_{ps} = 88 + 201gf + 401gd - 201g(h_i h_r) - K_n \quad (3)$$

In equation (3),  $h_r$  indicates the antenna height,  $h_t$  indicates the transceiver module height,  $f$  radio frequency,

$K_h$  environmental correction factor, and  $d$  indicates the distance between the transceiver and signal antennas.

**B. Construction of Time Delay and Energy Consumption Model of High Voltage Cable in Mountainous Areas**

The high-voltage cable monitoring model uses LoRa to achieve optimization of dynamic grouping with multiple objectives, and algorithms are used to find the number of cellular wireless modules installed as well as the number, so as

to achieve the type of network under different system delay and energy consumption conditions, and to meet the switching of multiple working states of the high-voltage cable monitoring system of smart grid. Network modeling is used in the study as a data directed graph, and transmission towers are located at substation locations, which can directly use LoRa modules to achieve end-to-end data transmission. Therefore, the directed graph then mainly considers the number of transmission towers required by the wireless transmission module. The directional diagram of network data transmission is shown in Fig. 3.

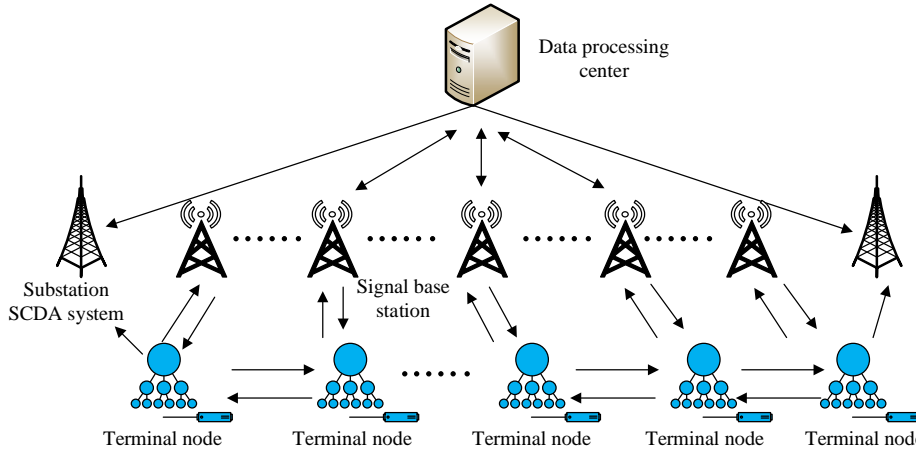


Fig. 3. Directed graph of network data transmission

The cable detection model mainly needs to find the available communication path and the communication link delay is kept minimum and can save the network construction cost, then the communication link delay should be less than or equal to the maximum communication delay, as seen in equation (4).

$$\sum_{(i,j)} D_{i,j,k} M_{i,j,k} \leq D_{\max} \quad \forall k \in N \quad (4)$$

In equation (4),  $M_{i,j,k}$  denotes the binary decision variable,  $D_{i,j,k}$  denotes the node  $k$  communication delay, and  $D_{\max}$  denotes the system maximum delay requirement. To ensure that the communication link is reused at a reduced cost, then  $O_{i,j}$  denotes the binary variable, if the data link  $(i, j)$  is used, there is  $O_{i,j} = 1$ , otherwise  $O_{i,j} = 0$ , expressed as seen in equation (5).

$$M_{i,j,k}, L_i, G_i, O_{i,j} \in \{0,1\} \quad \forall (i, j) \in p, \forall k \in N \quad (5)$$

In equation (5),  $L_i$  and  $G_i$  are binary variables, where  $i$  towers use cellular network, then there is  $G_i = 1$ , otherwise 0, and if  $i$  towers use LoRa, then  $L_i = 1$ , otherwise 0. The variables  $M_{i,j,k}$  and  $O_{i,j}$  can be determined by equation (5). Also combine equation (4) with equation (5) to get all network delay functions as seen in equation (6).

$$D(M_{i,j,k}, L_i, G_i, O_{i,j}) \quad \forall (i, j) \in p, \forall k \in N \quad (6)$$

The expression of the network loss function can be found by equation (6) as seen in equation (7).

$$E(G_i, L_i) = \sum_{i=1}^N (dG_i + bL_i) + \sum_{(i,j) \in p} C_{i,j} O_{i,j} + L_{ps} \quad (7)$$

In equation (7),  $d$  denotes the energy consumption of the cellular radio module,  $b$  denotes the energy consumption of the LoRa module, and  $C_{i,j}$  denotes the energy consumption at the data link  $(i, j)$ . The expression of the dynamic model of mountain cable LoRa obtained by Eq. (4) to Eq. (7) is seen in Eq. (8).

$$F[D(i, j, k), E(i, j)] \quad \forall (i, j) \in p, \forall k \in N \quad (8)$$

In the LoRa module,  $SF$  is the spreading factor,  $BW$  is the signal bandwidth, and  $CR$  is the encoding rate. Using the sem tech formula, the transmission time of a LoRa individual node packet over the air can be calculated, and by using the user key control parameters, the LoRa symbol rate is expressed as seen in equation (9).

$$R_s = \frac{BW}{2^{SF}} \quad (9)$$

With the user control parameters and the symbol rate definition information, the LoRa symbol period representation is obtained as seen in equation (10).

$$T_s = 1/R \quad (10)$$

The number of propagation times of LoRa data in the air is the sum of the packet transmission time and the leading code time, while the leading code is calculated as seen in equation (11).

$$T_p = (n_p + 4.25)T_s \quad (11)$$

In equation (11),  $n_p$  is the leading code setting length, which is stored in the register location, then the payload transmission time is equation (12).

$$T_l = \varepsilon * T_s \quad (12)$$

In equation (12),  $\varepsilon$  denotes the payload symbol, then the LoRa data transmission time can be obtained as the sum of the leading code transmission time and the payload time, as seen in equation (13).

$$T = T_p + T_l \quad (13)$$

In equation (13),  $T_p$  is the lead code transmission time,  $T_l$  is the payload time. LoRa data transmission process energy generation as seen in Figure 4.

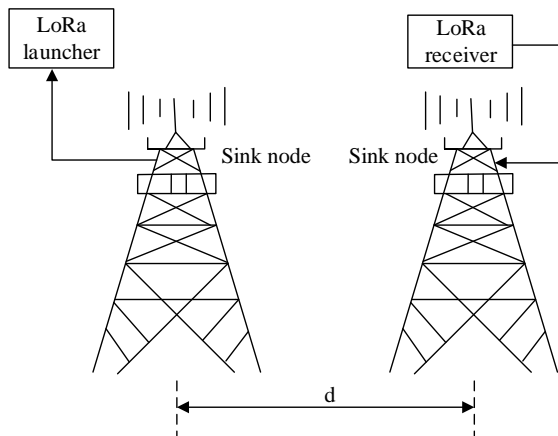


Fig. 4. Lora energy generation in lora data transmission process

Then, in LoRa data transmission,  $E_{RX}$  denotes the data transmitting energy consumption,  $E_{TX}$  denotes the data receiving energy consumption,  $d$  denotes the distance of data transmission process, and  $n$  denotes the data size. The total energy consumption of LoRa data transmission is shown in equation (14).

$$\begin{cases} T_{TX}(n, d) = E_{Telec} \times n + \varepsilon_{amp} \times n \times d^k \\ E_{RX(n)} = E_{RX-elec(n)} = E_{Relec} \times n \\ E_{LoRa} = E_{TX}(n, d) + E_{RX}(n) \\ E = L_{LoRa} + E_{CC}(n) \end{cases} \quad (14)$$

In equation (14),  $E_{Telec}$  is the energy consumption of the device sending data,  $E_{Relec}$  is the energy consumption of the device receiving data,  $\varepsilon_{amp}$  is the energy consumption of the device power amplifier unit,  $E_{CC}(n)$  is the energy consumption of the cellular module sending data, and  $k$  is the signal attenuation index with a value of 4 in the mountain area.

### C. Lora Transmission Model Construction based on MOPSO Algorithm

The analysis of the LoRa transmission model reveals that the delay model is influenced by the LoRa transmission data and device transmission parameters, while the energy consumption model is influenced by the data transmission distance, data transmission volume, and transceiver module power. Meanwhile delay and energy consumption are two contradictory target data. To ensure both low latency and good energy consumption for high voltage cable monitoring system, a compromise approach is needed. A neural network algorithm is used to optimize the delay and energy consumption objectives so that the delay and energy consumption targets meet the requirements of the online high-voltage cable detection system. Therefore, the multi-objective particle optimization algorithm (MOPSO) is used to optimize the energy consumption  $E$  and  $T$  two important parameter objectives, then the mathematical expression of MOPSO for  $M$  objectives is seen in equation (15).

$$\begin{cases} \min y = f(x) = |f_1(X), f_2(X), \dots, f_m(X)| \\ S.t. \quad x = (x_1, x_2, \dots, x_D) \in X \\ \quad \quad y = (y_1, y_2, \dots, y_M) \end{cases} \quad (15)$$

In Eq. (15),  $y$  denotes the target space,  $X$  denotes the decision space,  $y$  denotes the target vector, and  $x$  denotes the decision vector. In the multi-objective particle swarm algorithm calculation, each particle has a unique solution in the solution space and adjusts its target flight according to the

spatial flight experience of its peers and its own experience. The particle trajectory in space has the best flight position, which is the optimal solution for the particle swarm. And the flight position that the whole particle swarm experiences is the optimal solution that the swarm finally searches for.

Define  $H_a = (h_{a1}, h_{a2}, \dots, h_{aD})$  as the  $D$  dimensional position of the  $a$  particle of the particle swarm and the particle  $a = 1, 2, \dots, s$ . The flight speed of particle  $a$  is  $aV_a = (v_{a1}, v_{a2}, v_{a3}, \dots, v_{aD})$ . The optimal solution of the particle swarm  $a$  is  $p_a = (p_{a1}, p_{a2}, p_{a3}, \dots, p_{aD})$ , and the global optimal solution of the whole particle population is  $p_o = (p_{o1}, p_{o2}, p_{o3}, \dots, p_{oD})$ . The particle population counts the velocity expression of the particles in each iterative update as seen in equation (16).

$$v_{ab}(k+1) = \theta v_{ab}(k) + c_1 r_1 (p_{ab} - h_{ab}(k)) + c_2 r_2 (p_{gb} - h_{ab}(k)) \quad (16)$$

In Eq. (16), denotes the number of particle swarm,  $a = 1, 2, \dots, s$  and  $b$  are the parameter values,  $b = 1, 2, 3, \dots, D$  and  $L_b$  denote the lower limit of the search space,  $U_b$  denotes the upper limit of the search space,  $v_{ab}$  denotes the swarm flight speed,  $c_1$  and  $c_2$  denote the swarm learning factor,  $\theta$  denotes the inertia weight, and  $r_1$  and  $r_2$  denote the random number. For each iteration, the position of the particles is expressed as shown in equation (17).

$$h_{ab}(k+1) = h_{ab}(k) + v_{ab}(k+1) \quad (17)$$

In equation (17),  $h_{ab}$  is the particle swarm dimensional position,  $Dh_{ab} \in [L_b, U_b]$ . The flow of multi-objective particle swarm to achieve the objective optimization is shown in Fig. 5.

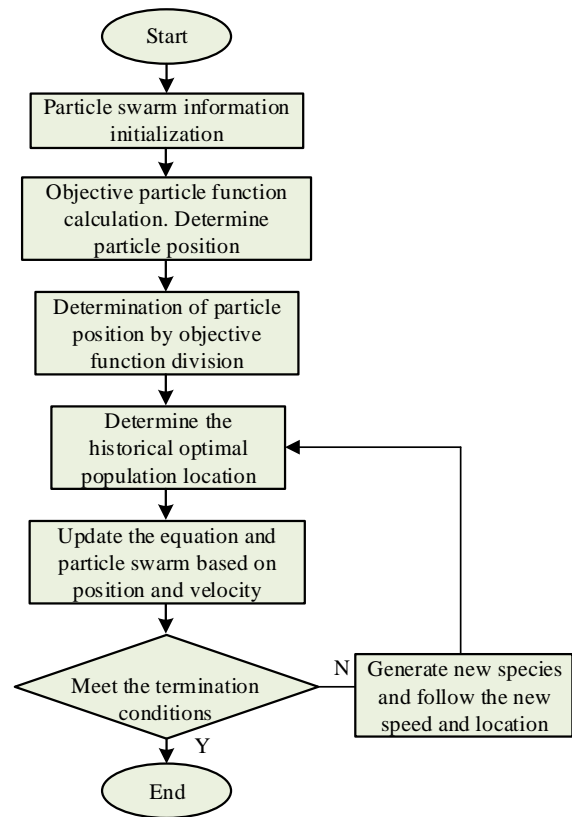


Fig. 5. Multi-objective particle swarm optimization process

### III. HIGH VOLTAGE CABLE CONDITION DETECTION MODEL SIMULATION TEST

In order to verify the performance of the proposed online high-voltage cable detection model, the online high-voltage cable monitoring network will be simulated and tested using MATLAB with Pocket Tracer simulation platform. The LoRa module used in the experimental test transmits from 1km to 5km range, and the transmission rate ranges from 5kb to 30kb range, and the distance is inversely proportional to the data transmission rate; while the cellular wireless module is used without considering the distance, and the rate is 125m/s. The cellular network has been affected by data access delay, routing conversion, and the delay is taken as the average value of 55ms. 100 transmission poles with a spacing of 1 km, and each inductive pole tower are placed a group of sensors, each group of sensors each time to collect data capacity of a total of 2.78kb.

In the test of the relationship between path loss and the influence of LoRa signal receiving and transmitting segment distance, the experiments are based on the Egli path loss model, and the relationship between path loss and LoRa signal segment is obtained through simulation tests, as shown in Fig. 6.

Fig. 6 shows the results of the relationship between the actual field strength of the path and the theoretical field strength. The real field strength test shows that the LoRa signal becomes weaker with the increasing distance of the field strength, which corresponds to the decreasing trend of field strength with increasing distance of Egli model. However, the actual comparison shows that the decreasing trend of field strength in the experimental test is significantly smaller than the trend of Egli's theoretical calculation. In the case of mountain peaks, the difference between the actual field strength and the theoretical field strength will be monotonically reduced by the increasing distance, but the error value will increase in the case of mountain peaks. Although the Egli model can describe the relationship between field strength and distance for transmission signals in mountainous areas, the model has a large error and needs to be optimized to effectively predict the path loss in mountainous areas. Meanwhile, in online high-voltage cable detection system, delay model and

energy consumption model are the key to system optimization. To discuss the performance of LoRa wireless networking, it is necessary to analyze the LoRa bottleneck energy in cellular wireless modules as well as the number of groups in LoRa modules and multi-hop transmission distance between modules. Therefore, the relationship between different wireless transmissions and the maximum system delay during networking is tested in the Pocket Tracer simulation platform, as shown in Fig. 7.

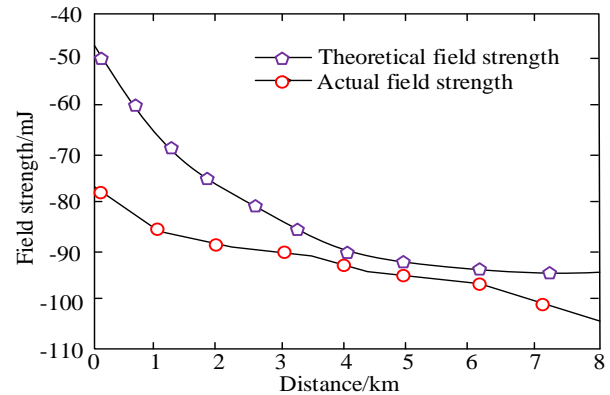


Fig. 6. It is the result of the relationship between the actual field strength and the theoretical field strength of the path

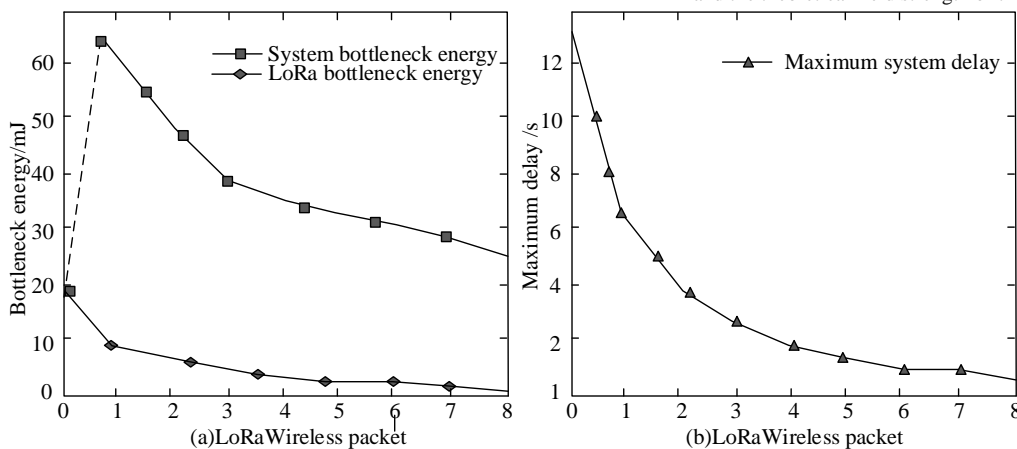


Fig. 7. Results of the relationship between system delay and bottleneck energy consumption

Fig. 7 shows the results of the relationship between the system delay and the bottleneck energy consumption. In Fig. 7(a) the results of the relationship between the number of LoRa wireless groups and the bottleneck energy are shown. When the cable monitoring network belongs to LoRa step-by-step hopping network, the system bottleneck energy is the same as LoRa bottleneck energy, and the terminal node closest to the gateway node transmission network will forward all node data at this moment, and the system bottleneck energy is consumed as the energy of this node; meanwhile, LoRa transmission group expands with the number, this network system takes cellular module for data transmission, and the cellular module energy consumption is much higher than the LoRa module, and the system bottleneck energy at this moment also increases with it. However, along with the expansion of the number of cellular modules, the transmission of data information of individual modules decreases, so the system bottleneck energy under the network will decrease as the number of module

groups increases. Also, when the system uses a heterogeneous network, LoRa modules will also consume less bottleneck energy as the number of LoRa groups increases. The bottleneck energy consumed by the LoRa and cellular networks is relatively fixed at this moment, with the LoRa bottleneck energy consumption being 2mJ and the cellular 27mJ. The results of the relationship between the number of wireless groups and the maximum delay are shown in Fig. 7(b).

Due to the increasing number of LoRa wireless packets, the data transmission between individual LoRa modules is reduced, and not only the energy consumption is reduced, but also the maximum delay of data transmission is gradually reduced.

The MATLAB platform is used to implement the simulation test for the multi-objective optimization of the system, and the multi-objective particle swarm algorithm is

used to optimize the two objectives of the delay module and the energy consumption module. The simulation test continues to reflect the results of the relationship between energy consumption and delay by bottleneck energy and maximum delay, as seen in Fig. 8.

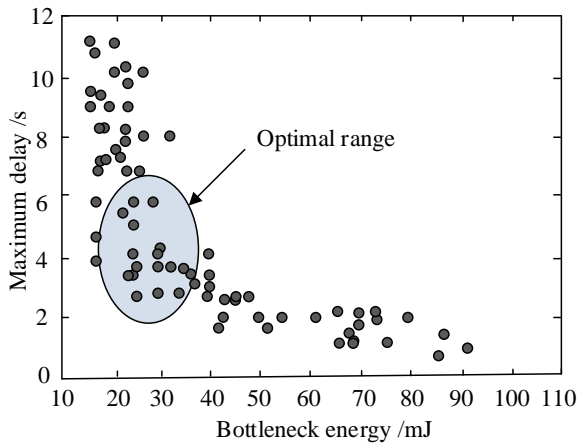


Fig. 8. Results of the relationship between time delay and energy consumption under particle swarm optimization algorithm

The results of the relationship between time delay and energy consumption under the particle swarm algorithm are shown in Fig. 8. The time delay and energy consumption are two conflicting objectives that show an inverse proportional relationship. Optimization of the two models of time delay and energy consumption by the multi-objective particle swarm algorithm does not search for the optimal solution set that matches the objective function. However, in the simulation test, the blue area of the image ellipse is the optimal solution range of the objective. In order to find the best working conditions parameters that meet the system work, it is necessary to further analyze the optimal solution set obtained by the particle swarm algorithm, and through the weighting process, the weights achieve the switching effect of working mode, and the normalization process is carried out to get the results corresponding to the parameters of time delay and energy consumption under different weights  $\omega$ , as shown in Table I.

TABLE I. SHOWS THE RESULTS OF TIME DELAY, ENERGY CONSUMPTION AND THE RELATIONSHIP BETWEEN PARAMETERS

Weight	Transmission distance/km	Signal bandwidth/K Hz	System energy consumption/mJ	System delay/s
0.1	1	125	12	9.13
0.2	1.5	125	14	5.01
0.3	2	125	25	2.72
0.4	2.6	125	32	0.91
0.5	3	125	48	0.53
0.6	3.5	250	53	0.47
0.7	4	125	59	0.36
0.8	4.5	250	71	0.26
0.9	5	250	74	0.16

Table I shows the results of time delay, energy consumption and the relationship between each parameter. At the weight of  $\omega=0.2$ , the system has the best balance of energy consumption and time delay, which can be used as the monitoring mode of cable detection system at this moment, and at  $\omega=0.5$ , the system has low delay and good signal transmission distance, which can be used as the warning mode of the system. At  $\omega=0.9$ , the system has the best delay performance and transmission distance, 0.16s and 5km, respectively, as maintenance mode. The proposed wireless inspection system can effectively meet the work content requirements of cable repair and maintenance, and the energy consumption is reduced by 81% compared with the traditional wired inspection system.

Packet loss rate is an important parameter to evaluate the quality of communication transmission, mainly refers to the ratio of the amount of data lost during the transmission and exchange process of communication data to the actual sent communication data. A higher packet loss rate means a worse quality of communication data transmission. Therefore, in order to ensure that the system communication has a high quality, it is necessary to consider the communication packet loss rate. The packet loss rate is related to the communication distance, packet length and the transmitting frequency of the signal base station. Therefore, the packet loss rate was tested under three detection models, and 2000 16-bit byte packets were sent simultaneously in the three operating modes of the system, as shown in Table II.

TABLE II. SHOWS THE RESULTS OF PACKET LOSS RATE OF THE SYSTEM UNDER VARIOUS WORKING MODES

System working mode	Total transmitted packets	Communication distance /kg	Packet loss rate	Time delay/s
Early warning mode	1950	3	<3%	0.51
	1956	3	<3%	0.52
	1972	3	<3%	0.53
Monitoring mode	1901	1.5	<5%	5.12
	1908	1.5	<5%	5.16
	1910	1.5	<5%	5.19
	1980	5	<1%	0.16
Maintenance mode	1982	5	<1%	1.17
	1986	5	<1%	1.17

Table II shows the results of the packet loss rate situation of the system under each operating mode. The packet loss rate of the system under all three modes tested is controlled within 5%, which meets the relevant requirements of packet loss rate for China's power grid communication construction. In the early warning mode and maintenance mode, the packet loss rate is significantly lower than that in the monitoring mode, mainly because the communication system needs to maintain high frequency signal bandwidth to meet the requirements of low delay in communication in both working environments, and therefore the energy consumption in both working modes



is relatively high. It can be concluded that the three working modes will be freely switched according to the environmental conditions where the high-voltage cable is located, maintaining the basic communication and low energy consumption detection requirements in the detection mode, and switching to the warning or maintenance mode under the harsh environmental conditions to guarantee the detection of the system and the exchange of communication data. Finally, compare the wireless cable detection technology studied with the traditional wired cable detection technology, as shown in Table III.

TABLE III. COMPARISON BETWEEN THE PROPOSED CABLE DETECTION TECHNOLOGY AND TRADITIONAL CABLE DETECTION TECHNOLOGY

Comparison type	Traditional cable detection technology	The proposed wireless cable detection technology
Scope of application	Only applicable to places where wired equipment can be built	It can adapt to most places, including high mountains, cold and hot areas
Unit energy consumption	higher	moderate
Self energy level system	Manual automatic control	Intelligent/manual control
Construction requirements	High construction difficulty, not suitable for all places	It can be built in most places and mobile communication coverage areas
Maintain	High maintenance difficulty and cost	Lower overall maintenance and cost
Check the accuracy	No time interval monitoring, and manual monitoring is required for special environment	Adapt to full time and assist manual monitoring, with higher detection accuracy

Table III is a comparison table between the proposed scheme and the traditional cable detection technology. It can be seen from the information in the table that compared with the traditional cable detection technology, the proposed wireless cable detection technology has obvious advantages in the scope of application, construction cost and detectability. At the same time, the cable detection technology based on wireless technology has more advantages than the traditional cable detection technology in terms of system updating and technology upgrading, and is more in line with the construction requirements of the existing smart grid.

#### IV. CONCLUSION

High-voltage transmission circuit is an important part of the grid system, and the reliability of high-voltage cables directly affects the safe operation of the grid system. Along with the development of interest communication technology, advanced wireless communication technology will provide important technical support for the development of smart grid. To address the problem of insufficient maintenance of traditional wired high-voltage cable detection system in remote mountainous areas, a high-voltage cable path state monitoring scheme using LoRa technology is proposed based on wireless sensor network. And three monitoring modes are proposed according to the fault types of high-voltage cables; the balance of energy consumption and delay of cable communication is achieved by

multi-objective particle swarm algorithm. The experimental results show that the system delay, energy consumption and signal bandwidth are different under different weight parameters, and the overall effect of the cable detection system can be improved by selecting the appropriate cable detection model according to the different weight of the cable detection area. When the weight is  $\omega=0.5$ , the system has low delay and good signal transmission distance. At this moment, the system adopts warning mode. At the weight  $\omega=0.9$ , the system signal and transmission distance are in the best state. At this moment, the system uses maintenance fuzziness for routine cable maintenance. Compared with the traditional cable detection system, the overall energy consumption of the proposed system is reduced by 81%. Finally, in the communication data transmission test, the packet loss rate of data transmission under the three working modes is less than 5%. The system reasonably selects the working model according to the environment and ensures that the system has excellent data signal transmission performance, and meets the cable fault detection requirements. Compared with the traditional wired cable detection technology, the wireless cable detection technology consumes less energy and can adapt to a more demanding detection environment. At the same time, the system uses neural algorithms to balance the system parameters, which makes the overall detection performance more stable and better. Therefore, the high voltage cable detection technology based on wireless sensor network meets the requirements of smart grid construction and ensures the timely and effective detection of high voltage cables. However, there are also shortcomings in this research. The wireless cable detection technology only considers the impact of mountain environment on technology. In the actual technology construction, more demanding environment needs to be considered. At the same time, the wireless technology needs to consider the regional communication coverage during the construction process, and the combination of wired and wireless technology is the most effective method at present.

#### REFERENCES

- [1] H. Xu, "Fastest adaptive estimation algorithms for topological structure errors in smart grid networks", *Computer Communications*, vol. 160, pp. 197-203, 2020.
- [2] O. Elsayed, J. Zarate-Roldan, A. Abuellil, et al. "Highly Linear Low-Power Wireless RF Receiver for WSN", *IEEE Transactions on Very Large-Scale Integration (VLSI) Systems*, vol. 27(5), pp. 1007-1016, 2019.
- [3] J. C. Wang, M. S. Liao, Y. C. Lee, et al. "On enhancing the energy harvesting performance of the photovoltaic modules using an automatic cooling system and assessing its economic benefits of mitigating greenhouse effects on the environment", *Journal of Power Sources*, vol. 376, pp. 55-65, 2018.
- [4] S. Chamanian, S. Baghaee, H. Ulsan, et al. "Implementation of Energy-Neutral Operation on Vibration Energy Harvesting WSN", *IEEE sensors journal*, vol. 19(8), pp. 3092-3099, 2019.
- [5] Kumar, Sudhir. "Compartmental Modeling of Opportunistic Signals for Energy Efficient Optimal Clustering in WSN", *IEEE Communications Letters*, vol. 22, pp. 173-176, 2018.
- [6] G. Tabella, N. Paltrinieri, V. Cozzani, et al. "Wireless Sensor Networks for Detection and Localization of Subsea Oil Leakages", *IEEE Sensors Journal*, vol. 21, pp. 10890-10904, 2021.
- [7] A. Xf, B. Gf, B. Pp, et al. "Environment-fusion multipath routing protocol for wireless sensor networks", *Information Fusion*, 2020, vol.

- 53, pp. 4-19, 2020.
- [8] B. Hu, Z. Sun, J. Liu, "Distributed time synchronization algorithm based on sequential belief propagation in wireless sensor networks", *Computer Communications*, vol. 176, pp. 119-127, 2021.
- [9] E. H. Houssein, M. R. Saad, K. Hussain, et al. "Optimal Sink Node Placement in Large Scale Wireless Sensor Networks Based on Harris' Hawk Optimization Algorithm", *IEEE Access*, vol. 8(99), pp. 19381-19397, 2020.
- [10] F. Lin, W. Dai, W. Li, et al. "A Framework of Priority-Aware Packet Transmission Scheduling in Cluster-Based Industrial Wireless Sensor Networks", *IEEE Transactions on Industrial Informatics*, vol. 16, pp. 5596-5606, 2020.
- [11] C. Zhan, Y. Zeng. "Aerial-Ground Cost Tradeoff for Multi-UAV-Enabled Data Collection in Wireless Sensor Networks", *IEEE Transactions on Communications*, vol. 68(3), pp. 1937-1950, 2020.
- [12] W. Wang, G. Tong, "Multi-path unequal clustering protocol based on ant colony algorithm in wireless sensor networks", *IET Networks*, vol. 9(2), pp. 56-63, 2020.
- [13] A. Verma, S. Kumar, P. R. Gautam, et al. "Fuzzy Logic Based Effective Clustering of Homogeneous Wireless Sensor Networks for Mobile Sink", *IEEE Sensors Journal*, vol. 20(10), pp. 5615-5623, 2020.
- [14] G. Jaber, R. Kacimi, LA. Grieco, et al. "An adaptive duty-cycle mechanism for energy efficient wireless sensor networks, based on information centric networking design", *Wireless Networks*, 2020, vol. 26, pp. 791-805, 2020.
- [15] W. Wang, N. Yu, Y. Gao, et al. "Safe Off-Policy Deep Reinforcement Learning Algorithm for Volt-VAR Control in Power Distribution Systems", *IEEE Transactions on Smart Grid*, vol. 11, pp. 3008-3018, 2020.
- [16] E. Pan, P. Dong, W. Long, et al. "Provincial Grid Investment Scale Forecasting Based on MLR and RBF Neural Network", *Mathematical Problems in Engineering*, pp. 1-12, 2019.
- [17] H. A. Ying, D. A. Lei, B. Ji, et al. "Power forecasting-based coordination dispatch of PV power generation and electric vehicles charging in microgrid", *Renewable Energy*, vol. 155, pp. 1191-1210, 2020.
- [18] S. Bhamidipati, K. J. Kim, H. Sun, et al. "Artificial-Intelligence-Based Distributed Belief Propagation and Recurrent Neural Network Algorithm for Wide-Area Monitoring Systems", *IEEE Network*, vol. 34, pp. 64-72, 2020.
- [19] P. Iliadis, S. Chapaloglou, A. V. Nesiadis, et al. "Smart energy management algorithm for load smoothing and peak shaving based on load forecasting of an island's power system", *Applied Energy*, vol. 238, pp. 627-642, 2019.
- [20] R. K. Jyotheeswara, N. Sudhakar, "A new RBFN based MPPT controller for grid-connected PEMFC system with high step-up three-phase IBC", *International Journal of Hydrogen Energy*, vol. 43, pp. 17835-17848, 2018.